Cement & Concrete Composites 31 (2009) 496–504

Contents lists available at ScienceDirect

Cement & Concrete Composites

journal homepage: www.elsevier.com/locate/cemconcomp

Slip effects in reinforced concrete beams with mechanically fastened FRP strip

Jae Ha Lee [a], Maria M. Lopez [b,*], Charles E. Bakis [c]

[a] Department of Civil and Environmental Engineering, 212 Sackett Building, The Pennsylvania State University, University Park, PA 16802, United States
[b] Department of Civil and Environmental Engineering, 231E Sackett Building, The Pennsylvania State University, University Park, PA 16802, United States
[c] Department of Engineering Science and Mechanics, 212 Earth-Engineering Sciences Building, The Pennsylvania State University, University Park, PA 16802, United States

ARTICLE INFO

Article history:
Received 17 April 2008
Received in revised form 10 April 2009
Accepted 14 April 2009
Available online 24 April 2009

Keywords:
FRP
Stress transfer
Analytical modeling
Mechanical testing
Slip

ABSTRACT

This investigation concerns the flexural behavior of reinforced concrete (RC) beams strengthened with a mechanically fastened pultruded FRP strip (MF-FRP beams). Twelve small size MF-FRP beams and two control RC beams were tested under flexural loading. The main failure mode observed in this experimental program was nail rotation and bearing damage under increasing flexural load, which resulted in FRP slip with respect to the soffit of the RC-beam and loss of stress transfer. Strain gage data and visual observations obtained during the experiments provided useful insight for developing a new procedure for estimating the nominal moment capacity of the MF-FRP beams. The proposed method is guided by experimental evidence pointing to the significance of nail rotation associated with flexural cracking in RC beams. The developed procedure, based on a "strain reduction factor" of 24%, is able to estimate the nominal moment capacity of the MF-FRP beams with good accuracy.

1. Introduction

Fiber-reinforced polymer (FRP) composites are rapidly gaining acceptance as a cost effective, durable means of strengthening reinforced concrete (RC) structures. In most cases reported to-date, wet-laid and pultruded FRPs have been adhesively bonded to RC structures using epoxy resins. While the epoxy bonding method can be highly effective, it can be limited by lengthy surface preparation and curing times as well as the possibility of bond failure at the interface between concrete and FRP [1]. To overcome these limitations, Lamanna et al. [2] developed a method of using powder-actuated nails to mechanically fasten specially-made, pultruded, hybrid-fiber FRP strips to flexural RC members for strengthening purposes (MF-FRP method). Several combinations of unidirectional glass fibers (rovings), carbon fibers (tows), continuous strand glass mat, and matrix materials were evaluated [3]. As a result of these investigations, a new type of multidirectionally reinforced pultruded FRP laminate now known as Safstrip™ was developed specifically for mechanical fastening to concrete. The distinguishing feature of this pultruded FRP strip versus typical pultruded laminates for strengthening RC structures is that bearing failures induced by mechanical fasteners are designed to be ductile in Safstrip™. Therefore, this type of laminate is an appropriate choice for the MF-FRP strengthening method. A detailed description of the Safstrip™ laminate is given by Lamanna [3]. Recent research has demonstrated the significant enhancements of strength in flexurally loaded MF-FRP beams in comparison to unstrengthened beams, without a substantial decrease in ductility as is generally observed with epoxy-bonded FRP (EB-FRP) strengthening [2–5].

Lamanna [3] and Bank et al. [6,7] developed an analytical model for predicting the flexural behavior of MF-FRP RC beams. The force-carrying capacity per fastener was used to predict the bearing failure and consequent reduction of stress transfer in the FRP strip. In this model, if the shear force on a fastener exceeds the defined force-carrying capacity, the associated section of FRP is assumed to slip with a constant fastener force equal to the defined capacity. The capacity of a fastener was obtained from pull-off tests, where the FRP was attached by one fastener to a concrete block. The analytical model agreed well with experimental results from small-scale rectangular beams and full-scale T-beams in terms of load capacity. However, predicted mid-span deflections were not in agreement with experimental results for the small-scale beams, indicating a deficiency in the moment–curvature relationship in those cases.

El Maaddawy and Soudki [8] developed an analytical model for predicting yield and ultimate flexural loads of one-way RC slabs strengthened with FRP strips (Safstrip™) anchored by bearing plates. The bearing plates clamped the FRP strip to the concrete using bolts running through the thickness of the slab at a few select positions (mainly at the ends), which is a fundamentally different anchoring approach than that used by Lamanna [3] and Bank et al. [6,7] in earlier investigations. The analytical model developed by El Maaddawy and Soudki uses an empirically-based "bond factor" to account for the slip between the concrete and FRP. The bond

* Corresponding author. Tel.: +1 814 865 9423; fax: +1 814 863 7304.
E-mail address: mmlopez@engr.psu.edu (M.M. Lopez).

0958-9465/$ - see front matter © 2009 Elsevier Ltd. All rights reserved.
doi:10.1016/j.cemconcomp.2009.04.008

factor is multiplied by the strain at the soffit of the concrete to determine the strain in the FRP. Values of the bond reduction factor ranged from 0.9 to 0.7. Using this bond factor approach, predictions of yield load of the slabs were consistently conservative (by up to 8%) while predictions of ultimate were mostly nonconservative (by up to 24%).

The present investigation aims to improve the prediction of the flexural behavior of MF-FRP beams by accounting for slip between the FRP and concrete caused by factors such as bearing failure and nail rotation. The proposed method is guided by experimental evidence pointing to the significance of nail rotation associated with flexural cracking in RC beams. Predictions of the nominal moment capacity of the beams used in the present investigation are made using Lamanna's method [3,6,7] along with the proposed method.

2. Experimental investigation

FRP strips attached to concrete blocks with one or two nails were pulled off to estimate the shear capacity of the concrete-FRP joint. RC beams with mechanically fastened strips were subjected to flexure tests to evaluate the effectiveness of the MF-FRP strengthening method. Observations made during these tests guided the development of a new model accounting for slip between the FRP and concrete caused by factors such as bearing failure and nail rotation.

2.1. Specimen description

Concrete blocks of 130 mm × 130 mm cross section and 260 mm length were cast for use in the pull-off tests (see Fig. 1). The as-received FRP material was cut into 25 mm wide by 355 mm long strips and fastened to the concrete blocks using one or two nails of 32 mm length (see Fig. 1). Reinforced concrete (RC) beams were designed and fabricated based on ACI 318-05 [9] to fail by yielding of the tensile reinforcement followed by crushing of the concrete in both the unstrengthened and strengthened cases. The beams had a depth of 20 cm, a width of 15 cm, a length of 152 cm, and depth of concrete cover (to the center of the flexural steel reinforcement) of 38 mm. The reinforcing ratio and stirrup size and spacing were chosen based on these dimensions (see Fig. 2). Steel nails were employed to attach the FRP strips to the beams and blocks. Steel anchor bolts were used in place of one pair of nails at opposite ends of the FRP strip in the "production" beam specimens in order to obtain superior strengthening effects and ductility.

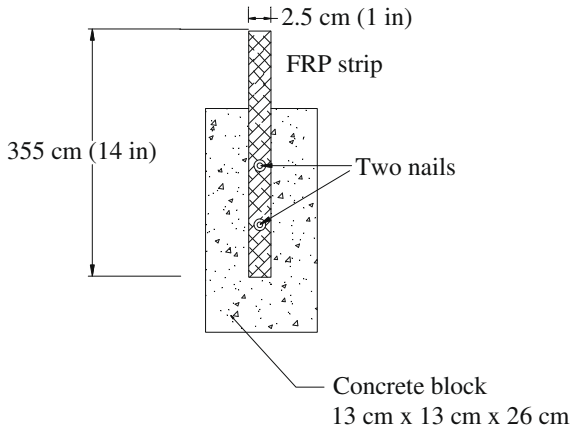

Fig. 1. Pull-off block specimen with FRP strip attached by two nails.

2.2. Material properties

A commercially mixed concrete with a 13 mm maximum aggregate size and 5% air entrainment was used for the blocks and beams. Grade 415 MPa deformed steel reinforcement bar was used. The Safstrip™ product discussed in the literature review was used for strengthening. The pultruded FRP strip, made by Strongwell (Bristol, VA, USA), is a hybrid carbon and glass fiber composite with vinylester matrix [3]. As manufactured, the strip is 102 mm wide and 3.2 mm thick. The properties of the concrete, steel bar and FRP strip were measured as a preliminary part of the investigation [10] and are listed in Table 1. Also, the bearing strength of the FRP strips was measured, according to ASTM D5961 [11], using nails and holes of 3.5 mm diameter. The load at the onset of bearing damage was found to be 3 kN, which translates to a 272 MPa bearing strength.

2.3. FRP pull-off test results

Fig. 3a illustrates the pull-off test set-up, which consists of a top plate and a bottom plate securing the concrete block using long threaded rods. Obtained load versus grip displacement graphs from the pull-off tests are shown in Fig. 4. On average, the maximum pull-off loads of concrete-FRP joints fastened with one and two nails of length 32 cm and diameter 3.5 mm were 6.10 kN and 11.7 kN, respectively. It was observed that the maximum pull-off load for one nail exceeded by a factor of two the 3 kN damage onset load of the bearing test. The cause of this apparent increase of bearing strength is hypothesized to be the rotation of the nail during the pull-off test and the consequent increase of clamping force acting through the thickness of the FRP strip near the nail. The appearance of extensive bearing failure of the FRP following a pull-off test is shown in Fig. 5a. The average pull-off load for two nails was approximately twice that for one nail. Additional experiments should be carried out to evaluate the maximum pull-off force for a larger number of nails.

2.4. Flexural behavior of MF-FRP beams

Three different types of MF-FRP beams and two control beams (i.e., no strengthening) were used for flexural testing. The fastener types and arrangements on three MF-FRP beams were varied at first in order to determine the most effective fastening scheme to be used in the remaining nine "production" beam specimens (beams 4–12). A description of the fasteners used for the MF-FRP beams, including nails and anchors, is given in Table 2. The 38 mm maximum nail length was limited by the depth of the concrete clear cover (22 mm) plus FRP thickness (3 mm) as suggested by previous research [3]. To prevent damage to the cover as the nails were inserted with a powder-actuated fastening tool, holes of 3 mm diameter were pre-drilled into the cover to a depth of 25 mm. The anchors, which screw into pre-drilled holes in the concrete, had a length of 54 mm and a diameter of 6.5 mm. Neoprene washers of 3 mm thickness were used to prevent damage to the FRP by the heads of the fasteners. Additional details of the fastening schemes are given by Lee [10]. Beams 1–3 and the two control beams were tested under 3-point loading (point load at midspan). The remaining MF-FRP beams (beams 4–12 in Table 2) were tested under a 4-point flexural load with a shear span length of 63.4 cm and an inner span of 15 cm, as shown in Fig. 3b) .

All flexure tests were conducted under displacement-control using a hydraulic actuator at a rate of 0.75 mm/min. Applied load, mid-span displacement and strain at several locations on the FRP strip were continuously recorded using a data acquisition system. The two control beams failed, as expected, by yielding of the longitudinal steel reinforcement followed by concrete crushing on the

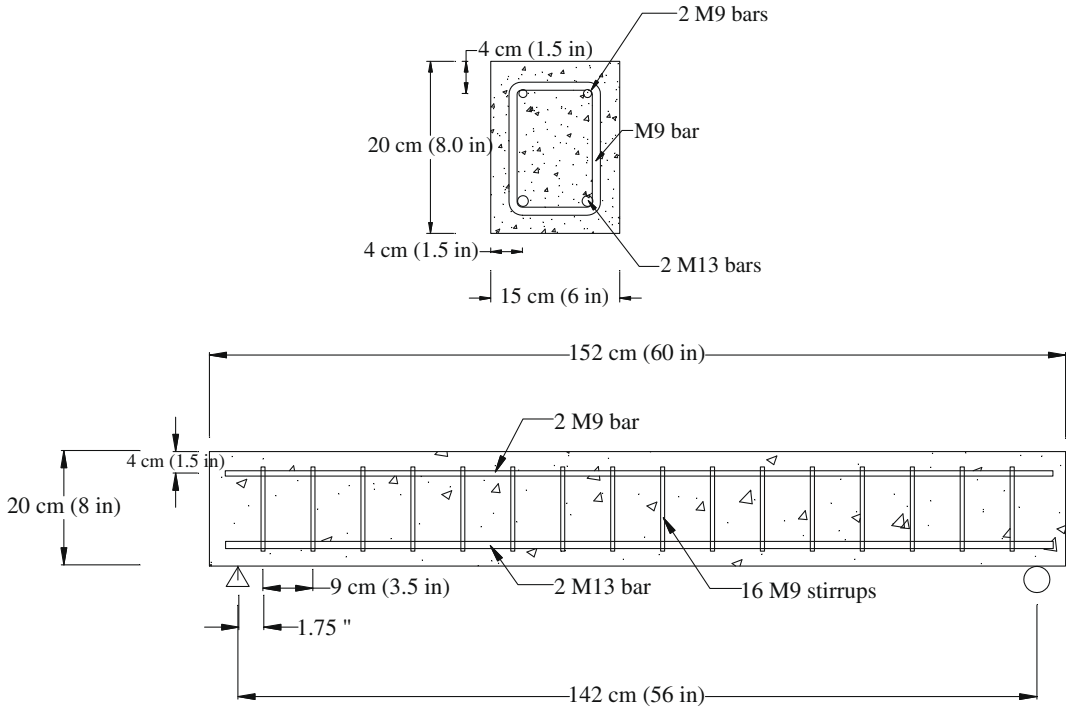

Fig. 2. (a) Cross-section of RC beam, and (b) reinforcement layout of RC beam.

Table 1
Measured material properties (concrete, steel reinforcement bar and FRP strip).

Concrete	Compressive strength (28th day) 28.8 MPa (4170 psi)		
Steel bar (#M13)	Elastic modulus 190 GPa (27,600 ksi)	Yield strain 0.0027	Yield stress 511 MPa (74.2 ksi)
FRP strip	Elastic modulus 68.3 GPa (9900 ksi)	Tensile strength 848 MPa (123 ksi)	Bearing damage onset[a] 269 MPa (39 ksi)

[a] Fastener and hole diameter = 3.5 mm.

compression zone. The average maximum moment at the midspan of the control beams was 21.0 kN m. Of the three differently strengthened MF-FRP beams, Beam 3 performed the best in terms of displacement-based ductility and strengthening effects, with a 35% increase in flexure strength and same ductility ratio when compared to the control beams, as shown in Table 3. Therefore, the fastening arrangement for Beam 3, as shown in Fig. 6 and Table 2 was used for the remaining beam experiments (beams 4–12).

The dominant failure mode of beams 3–12 was yielding of the longitudinal steel reinforcement followed by progressive concrete crushing concurrent with progressive delamination of the FRP strip. It was also observed from the flexural tests that the nails and anchors rotated with an increasing applied load even beyond concrete crushing. It appears that the presence of the nails and anchors acted as a crack initiator on the strengthened beams, in spite of the fact that all beams tested were precracked prior to installation of the MF-FRP system. Fig. 7 shows a photograph of a tested specimen. Limited bearing failure of the FRP strip only appeared in the vicinity of the anchors and nails near the supports. It is believed that the widening of concrete cracks that formed near the nails enabled the nails to rotate, thus minimizing the extent of bearing damage sustained by the FRP strip. Fig. 5b and c shows photographs of typical nail rotation and limited FRP bearing damage seen after flexural failure of a beam. Although the FRP strip slipped relative to the concrete during nail rotation and localized bearing damage, it remained attached to the soffit of concrete at the ultimate state, inducing a ductile flexural failure mode.

Fig. 6 shows the location of strain gages (SG1-4) along the surface of the FRP strip and the analyzed regions between the strain gages. Slip between the FRP and concrete was evaluated by comparing the average FRP strain distribution from beams 4 to 12 with the theoretical FRP strain distribution for the zero-slip case, at three different applied moments. Fig. 8 shows the comparison for the half-length of the beams. Both experimental and theoretical fully bonded curves showed a difference in the slope of the strain vs. position curve in the shear span (SG 1-3) versus the region between the 2-point loads (SG4). As expected, the largest strain values were obtained at midspan (SG4). SG3 values (both experimental and theoretical) were very similar to SG4 values, due to their proximity to the loading point. It is interesting to note that the experimental curves indicate a more gradual variation of strain versus position than the fully bonded case. It can be inferred that the slip created by the nail rotation and localized bearing failure lead to a more uniform strain distribution on the FRP. The presence of slip can be confirmed by the fact that all experimental strains were lower in magnitude than those for the fully bonded assumption, especially at the higher moments evaluated.

Strains recorded at the locations shown in Fig. 8 were used to determine the average force transferred per fastener in the regions between each pair of adjacent strain gages. For instance, the average transferred force for each nail in Region 2, N_2, is obtained by the imbalance of forces F_1 and F_2 existing at the sections of the FRP strip coincident with Gages 1 and 2, respectively, as seen in Fig. 9. The calculations are shown in Eqs. (1)–(4).

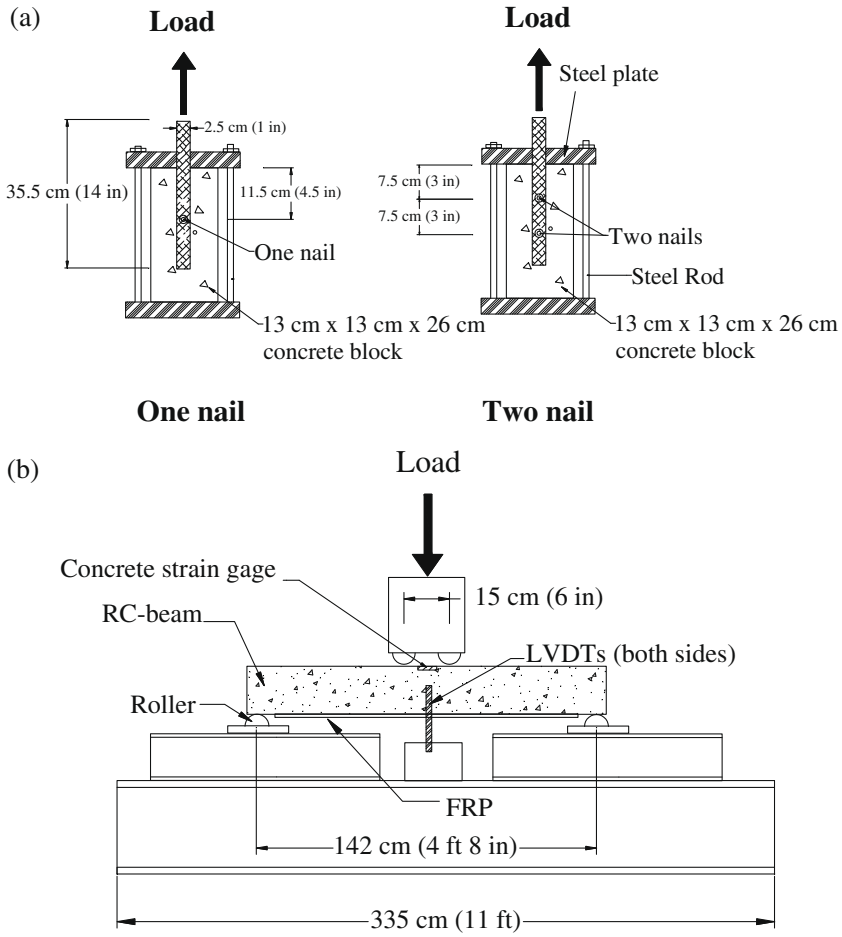

Fig. 3. Test setups for (a) pull-off test and (b) flexural test.

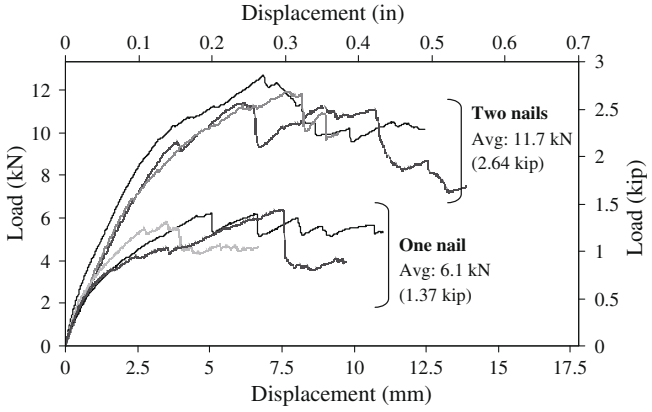

Fig. 4. Load versus displacement data for pull-off tests with FRP attached by one or two nails.

$$F_1 = \varepsilon_1 E_{FRP} A_{FRP} \quad (1)$$

$$F_2 = \varepsilon_2 E_{FRP} A_{FRP} \quad (2)$$

$$F_2 = F_1 + nN_2 \quad (3)$$

$$N_2 = \frac{(F_2 - F_1)}{n} \quad (4)$$

where ε_1, is the strain in SG1; ε_2, the strain in SG2; n, the number of nails in Region 2; A_{FRP}, the cross sectional area of FRP strip and E_{FRP}, is the elastic modulus of FRP strip.

In Region 1, one anchor is counted as two nails because its diameter is twice that of a nail.

The average force per nail for beams 4–12 is presented in Fig. 10. It can be observed that the force per nail (derived from experimental results) decreases as the distance to the point load decreases. This is the opposite trend of the "fully bonded" case, presented in Fig. 10 as well. This result is further evidence of how the lost of connectivity between nails and concrete, attributed to nail rotation and localized bearing failure, created a slip-enabled loss of force transfer in the regions closer to midspan (e.g. RG3, RG4) while increasing the "required" force transfer near the support (RG1).

Based on a comparison of results obtained from flexural and pull-off tests, it was ascertained that nail rotation is dependent on the type of specimen. Fig. 11 illustrates the different conditions of fastener anchorage in the beams and the blocks. In the case of the beams, as flexural loads are applied, crack width increases, allowing for relatively easy nail rotation. On the other hand, as pulling loads were applied to the block with FRP attached, it was observed that no cracks developed in the concrete. Indeed, the average force per single nail in the beam and in the block at ultimate condition, for each case, is 3.11 kN and 6.10 kN, respectively. Therefore, it would be incorrect to use the maximum force from pull-off tests to analyze the flexural behavior of the MF-FRP beams.

To assess the importance of nail rotation as a source of slip of the FRP strip relative to the concrete, slip as a function of position along the half-length of the strip at the ultimate state was estimated by observing the rotation of nails at several positions. Slip due to nail rotation was calculated based on the observed angle

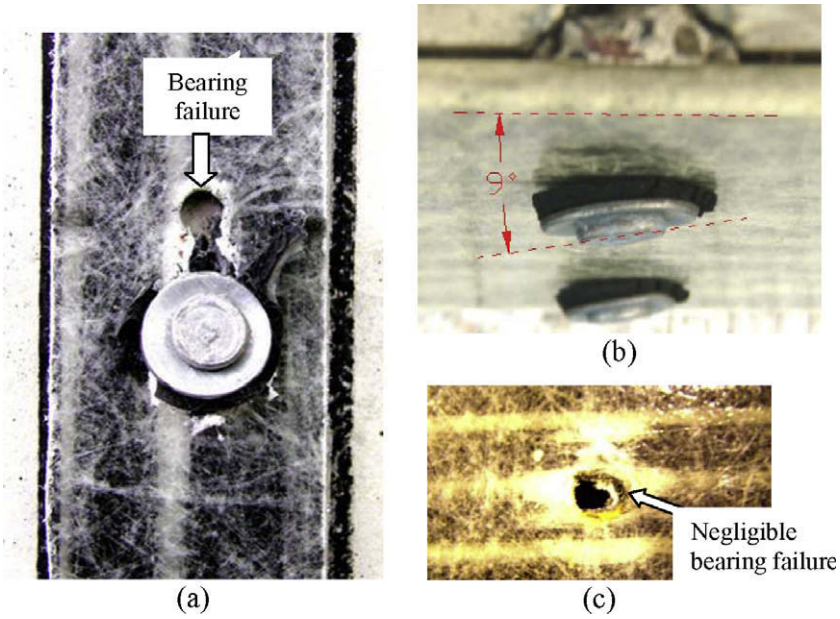

Fig. 5. Photographs of nail–FRP interactions: (a) extensive bearing failure after pull-off test; (b) nail rotation after flexure test; and (c) limited bearing failure after flexure test, after manual removal of nail for clarity.

Table 2
Description of fastening systems.

	Nail length (mm)	Nail diameter (mm)	Anchor length (mm)	Anchor diameter (mm)	Number of nails	Number of anchors
Beam 1	25	3.5	NA	NA	32	NA
Beam 2	32	3.5	NA	NA	32	NA
Beam 3	32	3.5	54	6.5	28	2
Beam 4–12	32	3.5	54	6.5	28	2

Table 3
Summary of test results for control beam and beams 1–3.

	Yield moment (kN m)	Ultimate moment (kN m)	Ductility ratio	Increase yield moment %	Increase ultimate moment %
Control beams (avg. of two specimens)	18.85	21.03	2.55	0	0
Beam 1	24.27	25.76	1.71	29	23
Beam 2	26.17	28.34	1.52	39	35
Beam 3	25.36	28.34	2.43	34	35

of the nail head as in Fig. 5b and the assumption of rigid body rotation of the nail (Fig. 12). These calculations, although approximate in nature, provide some insight on the contribution of nail rotation on the slip phenomenon. Other phenomena, such as unloading/rebound of the nails upon unloading, a small amount of bearing failure in the FRP strip and concrete, and deformation of the nails are likely to affect slip as well, based on visual observations.

3. Analytical investigation

Visual observations and measured strains have shown that slip and strain incompatibility due to fastener-related phenomena should be considered in the analysis of flexural behavior of the investigated MF-FRP beams. In the following discussion, strain incompatibility between the FRP and concrete is analyzed based on experimental data. Consequently, a procedure for estimating the nominal moment of the MF-FRP beam in consideration of strain incompatibility is proposed.

If we assume that the FRP strip is perfectly bonded to the soffit of the RC-beam and the shear capacity of the concrete cover is sufficient to carry the shear force induced by the tensioning of the strip, the strain at the mid-plane of the FRP strip (at midspan), ε_{FRP}, can be determined numerically based on strain compatibility, as shown in Eq. (5).

$$\varepsilon_{\mathrm{FRP}} = \varepsilon_c \left(\frac{d_{\mathrm{FRP}}}{c} - 1 \right) \tag{5}$$

where $\varepsilon_{\mathrm{FRP}}$ is the strain in the FRP strip, c the neutral axis depth, ε_c the strain in the concrete at the top of the beam, d_{FRP} is the distance from the extreme compressive fiber of the section to the mid-plane of the FRP strip.

However, due to fastener-related slip, strain in mechanically fastened FRP strips is less than that calculated assuming fully bonded conditions for any applied moment. This is clearly seen in Fig. 13, where experimentally measured strains at the midspan position of the strip are compared to theoretical strains based on the fully bonded assumption. It can also be seen that the ultimate moment obtained experimentally is approximately 60% of the nominal moment capacity at concrete crushing predicted using the fully bonded assumption. Hence, fastener-related slip causes an overall reduction of strengthening effectiveness of the FRP strip.

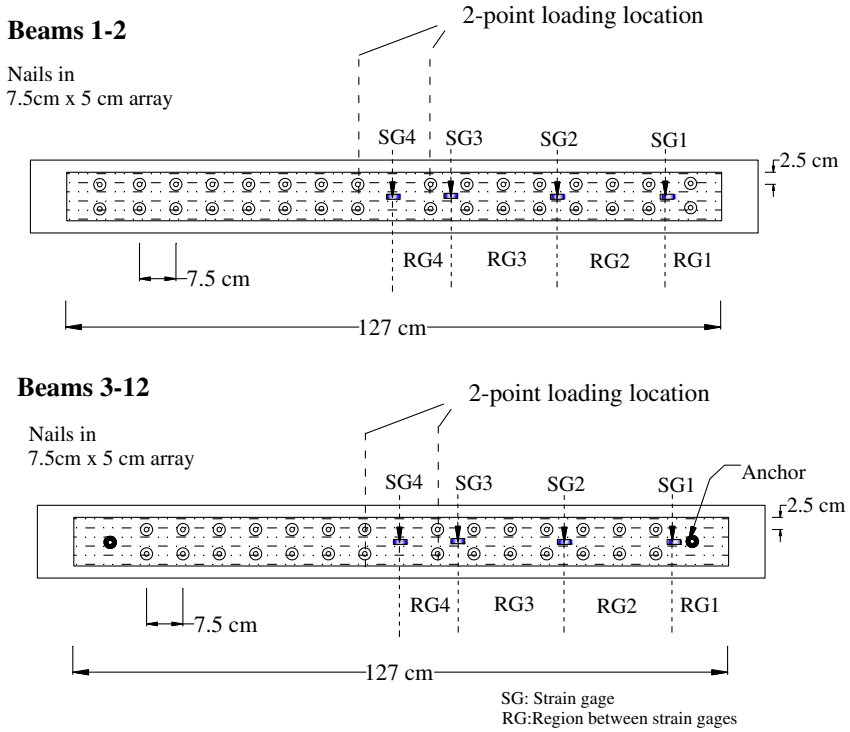

Fig. 6. Anchor, nail, region number (RG), and mounted strain gage (SG) number locations (beams 1–12).

Fig. 7. Photograph of flexure cracks near midspan in relation to the nail locations.

Based on the above findings, a reduction factor is introduced to take into account the effects of slip. Using an approach similar to that adopted by El Maaddawy and Soudki [8] for a different fastening scheme, the strain reduction factor is defined as the ratio of measured FRP strain at a given moment to predicted FRP strain based on the fully bonded assumption.

$$\text{Strain reduction factor} = \frac{\text{Measured FRP strain}}{\text{Predicted FRP strain based on fully bonded assumption}} \times 100\% \quad (6)$$

Using experimental data from beams 4 to 12, strain reduction factors were calculated for various applied moments. Fig. 14 shows a plot of the average strain reduction factor versus the concrete compressive strain at the top of the beam. The strain reduction factor decreases from 54% at the onset of loading to 22% at a concrete compressive strain of 0.0038. (It is noted that typical experimental values of concrete crushing strain ranged from 0.0016 to 0.0035.) The percent reduction of strain is maximized at the lowest applied moments because of initial slack in the fastening system (eg., lack of intimate contact between all bearing surfaces) rather than large slip distances. At high moments, conversely, slips are large while the percent reduction of strain is low. The minimum reduction factor of 22% near failure is substantially less than the 70–90% values proposed by El Maaddawy and Soudki [8] for yielding and ultimate conditions, reflecting the relatively less secure bond between the FRP strip and concrete in the present investigation. Recall that in Ref. [8] the FRP strip was actively clamped against the soffit by a bearing plate held by anchor bolts passing through the concrete slab.

A procedure for using the strain reduction factor to estimate the nominal moment capacity of the MF-FRP beam is described next. To begin the procedure, the MF-FRP beam is assumed to be fully

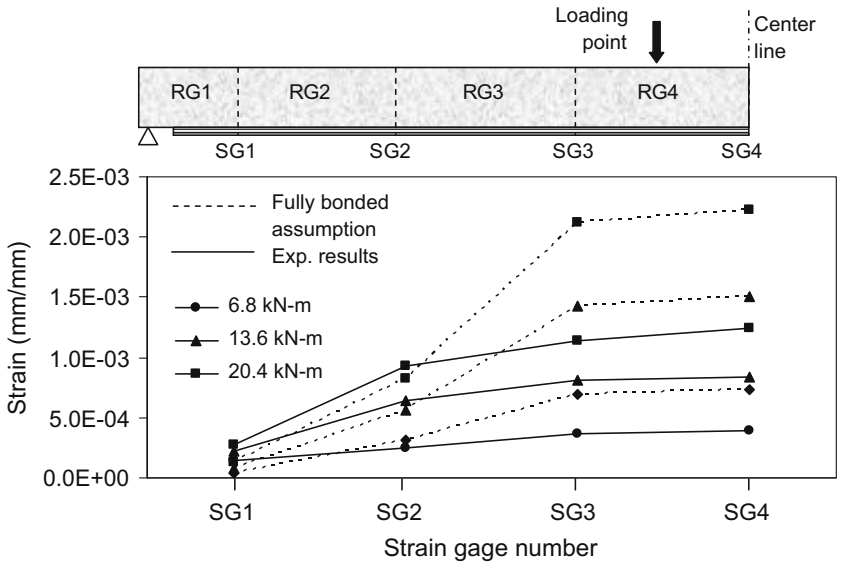

Fig. 8. Strain distribution in the FRP strip at three different levels of applied moment.

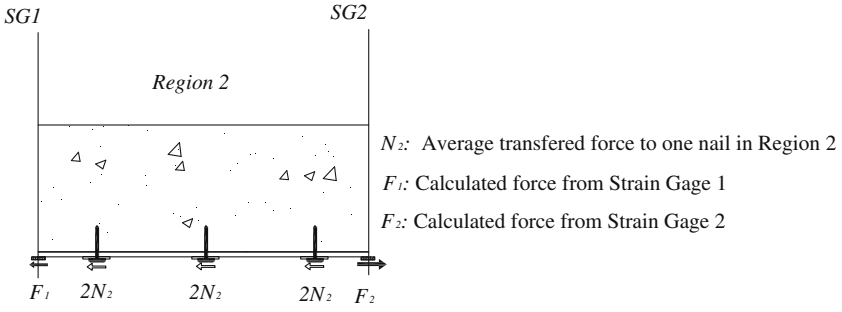

Fig. 9. Forces F_1, F_2, and N_2 acting on a segment of FRP sheet in Region 2.

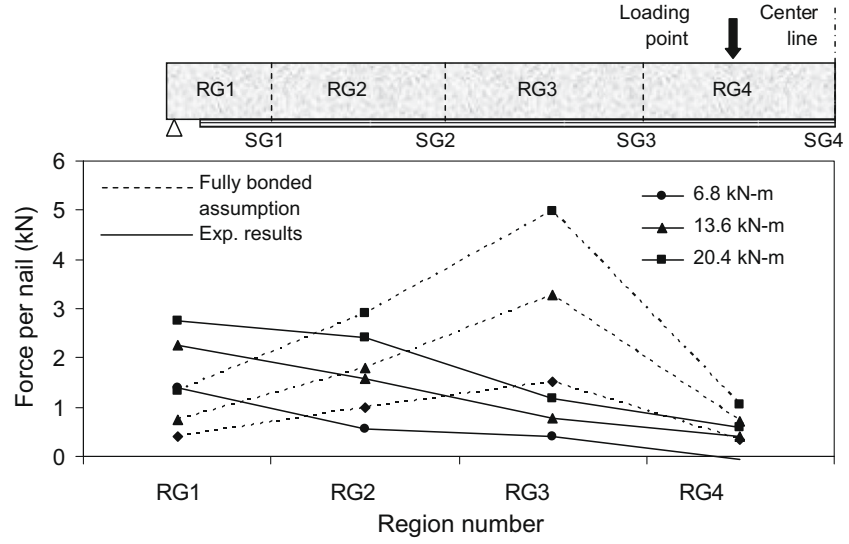

Fig. 10. Average force transferred per fastener in each region, based on strain data, compared with fully bonded assumption.

bonded. Based on this assumption, the neutral axis depth c is calculated. The strains in the FRP and steel bars are then calculated using the theory of strain compatibility. The strain in the FRP is then modified, using the strain reduction factor, to account for fastener and slip effects. In doing so, a revised c value is calculated to satisfy equilibrium of the section. Finally, the nominal moment is calculated using the revised c based on a concrete crushing strain of 0.003.

Individual strain reduction factors corresponding to the ultimate moment capacities of beams 4–12 are listed in Table 4. In

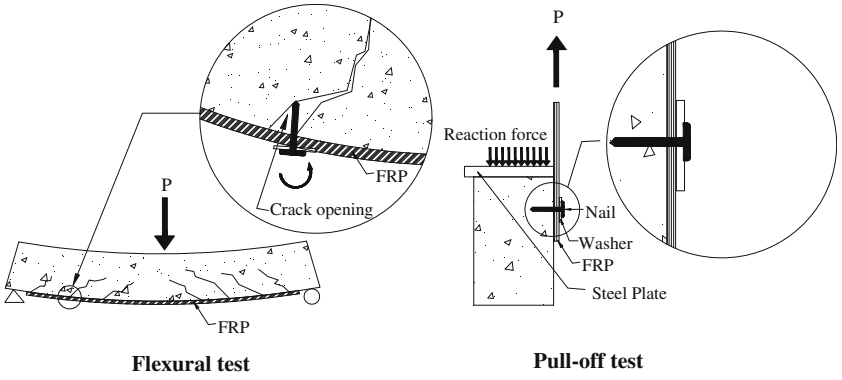

Fig. 11. Illustration of fastener loading conditions and nail movements in beams and blocks.

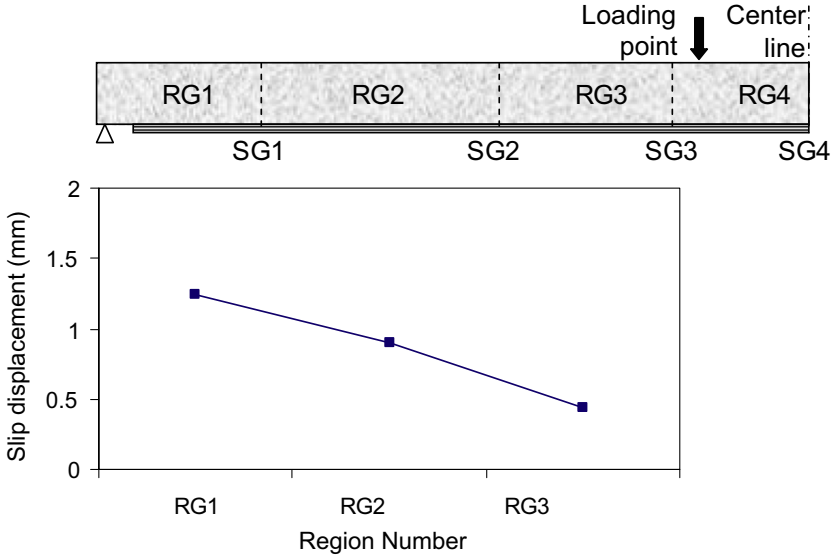

Fig. 12. Slip displacement of the FRP strip along the half-length of the beam after flexural testing, based on measured nail rotations.

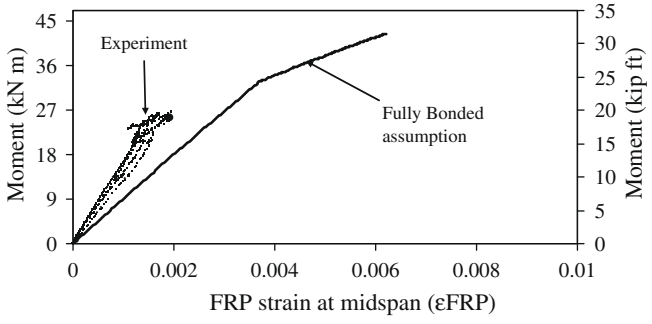

Fig. 13. Comparison of moment versus FRP strain at midspan: fully bonded assumption vs. experimental data. Curves are drawn to measured and nominal capacities.

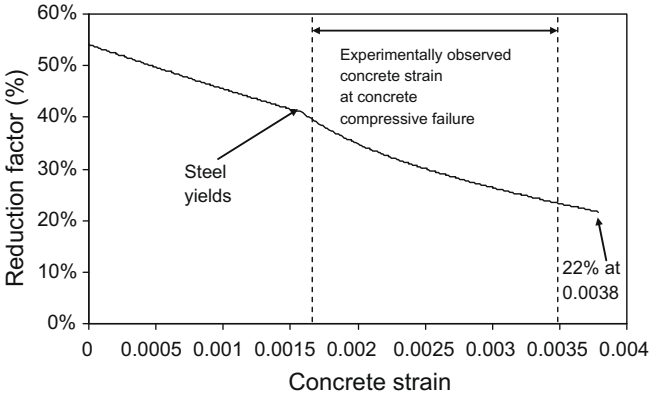

Fig. 14. Strain reduction factor vs. concrete strain at the top of the MF-FRP beam.

the interest of developing a design approach, the most conservative value of 24% was selected as the design strain reduction factor for the subject MF-FRP beams. The calculated nominal moment (at concrete crushing) and the corresponding strain of the FRP strip at midspan are 25.3 kN m and 0.00153, respectively, whereas the experimental average moment capacity and corresponding FRP strain based on beams 4–12 are 24.8 kN m and 0.00166, respectively. Therefore, by following the proposed procedure using the 24% strain reduction factor, the nominal moment of the beam and strain of the FRP strip were estimated to within 2% and 8% of the respective experimental values. As expected, the high degree of accuracy obtained was related to the use of experimental data to obtain the reduction factor.

It is illuminating to compare the proposed approach for predicting the strength of MF-FRP beams to another approach in the liter-

Table 4
Strain reduction factors at ultimate, based on Eq. (6).

Beam	Strain reduction factor (%)
4	33
5	33
6	31
7	39
8	32
9	24
10	26
11	31
12	30
Lowest value (design)	24

Table 5
Comparison of moment capacities calculated by various methods.

	Moment (kN m)	FRP strain	% *M*-error[a]
Experimental average	24.8	0.00166	0
Fully bonded assumption	42.8	0.00638	73
Lamanna's method	36.5	0.0044	47
Proposed nominal capacity based on strain reduction method	25.3	0.00153	2

[a] $\%\ M\text{-error} = (M - M_{experiment})/M_{experiment} \times 100$.

ature. Lamanna and Bank et al. [3,6] proposed a procedure to determine the strength of MF-FRP beams using a moment–curvature relationship based on a fully bonded condition. In this procedure, if the force required per fastener exceeds the maximum allowed force per fastener, it is assumed that a bearing failure occurs in the FRP strip. The maximum allowed fastener forces in Lamanna's procedure are derived from block pull-off tests rather than beam tests. Using the results from the pull-off tests of the present study, where the maximum load per nail was 6.10 kN, the failure moment and FRP strain at FRP bearing failure, according to Lamanna's method, are 36.1 kN m and 0.0044, respectively. Lamanna's model predicts FRP bearing failure prior to obtaining concrete crushing failure. The nominal moment at concrete crushing did not change significantly (36.5 kN m) as it is assumed that after bearing failure the FRP load is constant. In light of the experimental evidence obtained in the present investigation, the nominal moment by Lamanna's procedure was overly optimistic due to the fact that the assumed force capacity of the nails was roughly two times that measured *in situ* on the strengthened beams (3.11 kN). Table 5 compares moment capacities from experiments, the fully bonded assumption, Lamanna's method, and the proposed strain reduction factor method.

4. Conclusions

The quantitative results presented in this paper are limited to the reported materials, fastening details, and specimen geometry. The proposed generic approach for calculating FRP strains and nominal strength of the beam using the strain reduction factor should be applicable to other situations once the effects of parameters such as beam and FRP dimensions, reinforcing ratio, material properties, loading rate, and fastener details on the strain reduction factor have been determined. Based on the experimental and analytical investigations conducted in this study, the following specific conclusions are drawn:

1. The use of an anchor near the ends of the FRP strip proved to be highly effective for strengthening as it significantly enhanced the ductility of the MF-FRP beams. Likewise, longer fasteners increased the effectiveness of the strengthening.
2. Based on experimental strain data, progressive slipping of the FRP strip under increasing flexural load was able to be characterized. Factors such as rigid body rotation of the fasteners, as well as localized bearing failure and fastener deformation are believed to influence slip.
3. From the pull-off tests and flexural tests conducted in this study, it was found that the force-carrying capacity of the fasteners depends on the loading situation. In the case of beams, widening flexural cracks enabled a slip mechanism induced by nail rotation. Consequently, strain in the FRP strip was reduced relative the fully bonded situation and the force capacity of the nails was reduced relative to that seen in pull-off tests.
4. Experimental strains in the FRP strip and the ultimate moment capacity of the MF-FRP beams were smaller than predicted by the fully bonded assumption. Therefore, it is concluded that slip accommodated by nail rotation decreased the strengthening effectiveness.
5. The proposed strain reduction factor used for the downward adjustment of strains in the FRP strip versus the strains predicted by the fully bonded assumption varied from 54% at the onset of loading (where the effect of slack in the mechanically fastened connections is significant) to 24% at the nominal moment governed by concrete compression failure.
6. A method was developed to estimate the nominal moment of the MF-FRP beams and the corresponding FRP strain using the strain reduction factor. Taking into account the experimentally determined effects of slip, the nominal moment and strain of the FRP were calculated with good accuracy.

Acknowledgements

The authors gratefully acknowledge the support of the Korean Science and Engineering Foundation provided in the form of a fellowship, and the support of Strongwell Company that provided the FRP materials used in this study. Any opinions, findings, and conclusions or recommendations expressed in this paper are those of the authors and do not necessarily reflect the views of the sponsors.

References

[1] Coronado CA, Lopez MM. Sensitivity analysis of reinforced concrete beams strengthened with FRP laminates. J Cem Concr Compos 2006;28(1):102–14.
[2] Lamanna AJ, Bank LC, Scott DW. Flexural strengthening of reinforced concrete beams using fasteners and fiber-reinforced polymer strips. ACI Struct J 2001;98(3):368–76.
[3] Lamanna AJ. Flexural strengthening of reinforced concrete beams with mechanically fastened fiber reinforced polymer strips. PhD thesis, University of Wisconsin: Madison; 2002.
[4] Lamanna AJ, Bank LC, Scott DW. Flexural strengthening of reinforced concrete beams by mechanically attaching fiber-reinforced polymer strips. J Compos Constr 2004;8(3):203–10.
[5] Tang KH, Saha MK. Mechanically fastened FRP-strengthened RC beam under cyclic loading. In: Triantafillou TC, editor. Proceedings 8th symposium on fiber reinforced polymer reinforcement for concrete structures, FRPRCS-8. Patras: University of Patras; 2007. [Paper 9-3].
[6] Bank LC, Borowicz DT. Mechanically fastened FRP strengthening of large scale RC bridge T beams. Adv Struct Eng 2004;7(6):525–37.
[7] Bank LC, Arora D. Analysis of RC beams strengthened with mechanically fastened FRP (MF-FRP) strips. Compos. Struct. 2007;79(2):180–91.
[8] El Maaddawy T, Soudki K. Flexural strengthening of reinforced concrete slabs with mechanically-anchored unbonded FRP system. In: Triantafillou TC, editor. Proceedings 8th symposium on fiber reinforced polymer reinforcement for concrete structures, FRPRCS-8. Patras: University of Patras; 2007. [Paper 9-2].
[9] ACI Committee 318. Building code requirements for structural concrete (318-05) and commentary (318R-05). Farmington Hills: American Concrete Institute; 2005.
[10] Lee JH. Effect of sustained loads and environment on mechanically fastened FRP beams. MS thesis, University Park, The Pennsylvania State University; 2006.
[11] ASTM D 5961. Standard test method for bearing response of polymer matrix composite laminates. West Conshohocken: American Society for Testing and Materials; 2005.